

Thoracic outlet syndrome in 3T MR neurography—fibrous bands causing discernible lesions of the lower brachial plexus

P. Baumer · H. Kele · T. Kretschmer · R. Koenig ·
M. Pedro · M. Bendszus · M. Pham

Received: 10 July 2013 / Revised: 10 September 2013 / Accepted: 6 October 2013 / Published online: 22 November 2013
© European Society of Radiology 2013

Abstract

Objectives To investigate whether targeted magnetic resonance neurography (MRN) of the brachial plexus can visualise fibrous bands compressing the brachial plexus and directly detect injury in plexus nerve fascicles.

Methods High-resolution MRN was employed in 30 patients with clinical suspicion of either true neurogenic thoracic outlet syndrome (TOS) or non-specific TOS. The protocol for the brachial plexus included a SPACE (3D turbo spin echo with variable flip angle) STIR (short tau inversion recovery), a sagittal-oblique T2-weighted (T2W) SPAIR (spectral adiabatic inversion recovery) and a 3D PDW (proton density weighted) SPACE. Images were evaluated for anatomical anomalies compressing the brachial plexus and for abnormal T2W signal within plexus elements. Patients with abnormal MR imaging findings underwent surgical exploration.

Results Seven out of 30 patients were identified with unambiguous morphological correlates of TOS. These were verified by surgical exploration. Correlates included fibrous bands ($n=5$) and pseudarthrosis or synostosis of ribs ($n=2$). Increased T2W signal was detected within compressed plexus

portion (C8 spinal nerve, inferior trunk, or medial cord) and confirmed the diagnosis.

Conclusions The clinical suspicion of TOS can be diagnostically confirmed by MRN. Entrapment of plexus structures by subtle anatomical anomalies such as fibrous bands can be visualised and relevant compression can be confirmed by increased T2W signal of compromised plexus elements.

Key Points

- MR neurography (MRN) can aid the diagnosis of thoracic outlet syndrome (TOS).
- Identifiable causes of TOS in MRN include fibrous bands and bony anomalies.
- Increased T2W signal within brachial plexus elements indicate relevant nerve compression.
- High positive predictive value allows confident and targeted indication for surgery.

Keywords TOS · Thoracic outlet syndrome · MRI · MR neurography · Fibrous band

Abbreviations

TOS	Thoracic outlet syndrome
MRN	Magnetic resonance neurography
ENG	Electroneurography
EMG	Electromyography
PDW	Proton density weighted
SPACE	3D turbo spin echo with variable flip angle
STIR	Short tau inversion recovery
SPAIR	Spectral adiabatic inversion recovery

Introduction

The thoracic outlet syndrome (TOS) complex comprises three related disorders with affection of the neurovascular bundle in

P. Baumer (✉) · M. Bendszus · M. Pham
Department of Neuroradiology, Heidelberg University Hospital,
Im Neuenheimer Feld 400, 69120 Heidelberg, Germany
e-mail: philipp.baeumer@med.uni-heidelberg.de

H. Kele
Centre for Neurology and Clinical Neurophysiology, Neuer Wall,
Hamburg, Germany

T. Kretschmer
Department of Neurosurgery, Oldenburg Evangelical Hospital,
Oldenburg University, Oldenburg, Germany

R. Koenig · M. Pedro
Department of Neurosurgery, Ulm University Hospital/
Bezirkskrankenhaus Guenzburg, Günzburg, Germany

its pass through the costoclavicular space: classic TOS, vascular TOS and non-specific TOS [1]. Two of these, classic TOS and non-specific TOS, lead to neurological symptoms. Classic TOS (true neurological TOS or neurogenic TOS) is caused by compression of spinal nerves C8 and Th1 or the inferior trunk of the brachial plexus, often by a taut fibrous band which classically extends from a rudimentary cervical rib or elongated transverse process to the first thoracic rib [2, 3]. Compression of these lower parts of the brachial plexus leads to weakness and wasting of the thenar and hypothenar eminence, the ulnar hand intrinsic muscles and in severe cases the medial forearm muscles [4]. Sensory abnormalities including pain and paraesthesiae of the medial arm and forearm may be less pronounced in classic TOS. Therapy of classic TOS entails surgical sectioning of the fibrous band and in some approaches also of the cervical rib or the first rib [4, 5]. Contrary to classical TOS, non-specific TOS (or disputed TOS) has been a controversial subject and no consensus exists regarding the underlying pathology of non-specific TOS. Sensory complaints are generally reported as the predominant manifestation but motor weakness is also commonly described [5, 6]. Proposed therapies range from conservative treatment with specific physical therapy to surgical removal of the first thoracic rib and adjacent muscles [5–7].

Definitive diagnosis is notoriously difficult in both classic TOS and non-specific TOS. Differential diagnoses include motor neuron diseases, ulnar or median neuropathy, C8 radiculopathy, other brachial plexus lesions from neoplasms or inflammatory lesions. Electrophysiological studies play an important role in differentiating these conditions. Imaging studies have so far not offered significant aid in the diagnosis of TOS. Radiography is usually performed to confirm or exclude the presence of a cervical rib [8] but the presence of a cervical rib is not specific for a diagnosis of TOS since it has a prevalence of 0.7–1.6 % in the general population [9, 10]. Therefore, detection of more specific pathomorphological correlates for the confirmation of this entity is desirable.

Technical advances in magnetic resonance imaging (MRI) pulse sequences and higher field strength now allow for detailed imaging of the peripheral nervous system, also termed MR neurography (MRN) [11–13]. The typical MRN criterion for a nerve lesion is increased signal on T2 weighted (T2W) images confined to the site of the nerve lesion [14, 15]. The brachial plexus is an especially important target for MRN [16] since it is only with difficulties accessible to neurophysiological examination. In this investigation, we tested whether an optimised MRN protocol for the brachial plexus using custom-made surface coils was able to detect pathomorphological correlates of TOS, and whether these imaging correlates could then be confirmed by surgery.

Materials and methods

This prospective study was approved by the Ethics committee of the Medical Faculty of Heidelberg University (S-057/2009) and written informed consent was obtained from all participants. The inclusion criterion was a clinical diagnosis or at least high suspicion of classic TOS or non-specific TOS, with ENG (electroneurography)/EMG (electromyography) ruling out radiculopathy or any peripheral neuropathy located further distal than the plexus level. Exclusion criteria were previous surgery at the brachial plexus, including previous surgery for TOS or known tumour or any other mass lesion in or near the brachial plexus. Out of 36 patients examined, 4 were excluded because of previous TOS surgery, 1 because of post-surgical pressure palsy with pseudoneuroma formation and 1 because of subsequently diagnosed inflammatory neuropathy, leaving 30 patients (19 women, 11 men; age 40.7 ± 12.9 years) in the study group.

Patients were examined at the Department of Neuroradiology of Heidelberg University Hospital, between 08/2010 and 10/2012. MRN examinations were carried out on a 3-T unit (Magnetom VERIO; Siemens, Erlangen, Germany). All patients received the same examination protocol, which was specifically developed for imaging of the brachial plexus from the spinal nerve root level to the most distal levels in the axilla (Tables 1).

The protocol was designed in the following way: the SPACE (3D turbo spin echo with variable flip angle) STIR (short tau inversion recovery) sequence provided a bilateral overview of the brachial plexus and the cervical and upper thoracic spine. The T2W SPAIR (spectral adiabatic inversion recovery) was best for displaying nerve lesions, while the PDW (proton density weighted) SPACE gave a 3D view of plexus continuity and surrounding tissue. The latter two sequences were acquired using a custom-designed coil dedicated for high-resolution imaging of the supra-, retro- and infra-clavicular brachial plexus (NORAS, Würzburg, Germany). This is a two-element 2 x 4-channel surface coil (clothes-pin-coil) positioned on the corresponding body surface on the symptomatic side. Multi-planar image reconstruction was possible on the T2W SPACE STIR sequence as well as the PDW SPACE sequence with isotropic voxel size. Contrast agent was not administered unless clinical examination indicated additional vascular compression. Reliable discrimination of vessels against nerves was possible by their hyperintense signal and tubular winded course which was assessed slice-by-slice on the T2W SPAIR sequence and, if necessary, on PDW SPACE.

The evaluation of MR images was performed by two neuroradiologists (P.B., M.P.) with more than 4 and 7 years of training in MRN, respectively. Additional three-dimensional image evaluation and reconstruction was undertaken by these two readers since standard reconstruction in axial and sagittal orientation does not reliably allow identification of

Table 1 MRI sequences

Sequence	TR	TE	TI	Slice thickness	Pixel spacing	FoV	matrix	Slices	Averages	Coil
3D SPACE STIR coronal	3,800	267	180	0.8	0.78×0.78	250	320/314	72	2	Neck (SIEMENS)
T2W SPAIR sagittal-oblique	5,530	45		3.0	0.47×0.47	150	320/198	51	4	Dedicated surface coil (NORAS)
3D PDW SPACE coronal	1,170	33		0.7	0.70×0.70	180	256/258	51	2	Dedicated surface coil (NORAS)

subtle abnormalities of the brachial plexus and its surrounding tissues. Images were evaluated for anatomical anomalies such as bony extensions of cervical vertebrae or cervical ribs and hypointense fibrous bands extending from these, which are known to predispose for TOS. The brachial plexus was assessed at every level from spinal nerves to plexus cords for potential compression by adjacent structures and for signal changes on T2W indicative of nerve lesions. Only patients with positive MRN findings were subsequently surgically explored.

Results

Out of 30 patients included in this study, seven (23 %) displayed unambiguous findings in MRN as pathomorphological correlates of TOS (Table 2). A T2W lesion selective to the compressed plexus elements was detected in all of these patients (Figs. 1, 2 and 3). Four of them were cases of classic TOS (patients 1, 2, 4 and 5) and three had symptoms of non-specific TOS (patients 3, 6 and 7). In five (patients 1, 2, 3, 4 and 7), a fibrous band was detected which originated from a cervical rib in three cases. One patient had a pseudarthrosis between a cervical rib and the first rib, another had a synostosis between the first and second rib.

Ultrasound was not part of the standard diagnostic work-up of the study but was able to show a compression of the relevant plexus elements in four patients (patients 2, 4, 5 and 7). Fibrous bands were suspected by ultrasound in three of these cases but were depicted clearly only on MRN.

Surgery subsequently confirmed positive MRN findings (Figs. 4 and 5). All operated patients showed significant improvement in their symptoms.

In the remaining 23 patients with clinical diagnosis or suspicion of TOS, MRN did not detect abnormalities, and surgical exploration was to our knowledge not performed.

Discussion

The results reported here demonstrate that MRN can indeed detect specific findings to confirm a diagnosis of TOS. Two diagnostic criteria are helpful in the imaging diagnosis: (1) the

detection of an anatomical structure compressing the lower part of the brachial plexus and (2) the presence of an associated abnormal focus on T2W within the compressed plexus portions but sparing the upper plexus. Both criteria were positive in seven of 30 patients described here. Imaging findings were subsequently confirmed by the diagnostic “gold-standard” of surgical exploration of the lower brachial plexus and followed by resection of the anatomical structure responsible for entrapment.

In five out of seven cases, a fibrous band was found compressing the lower parts of the proximal brachial plexus. The occurrence of fibrous bands as compressive structures was reported by Thomas and Cushing in 1903 [2] and has since been observed regularly in situ by anatomists and surgeons [3, 9]. The reliable confirmation of the presence of a compressive fibrous band has to our knowledge not been achieved previously. The detection by MRN in our patients was made possible by specially designed surface coils and an optimised protocol devised for imaging of the brachial plexus.

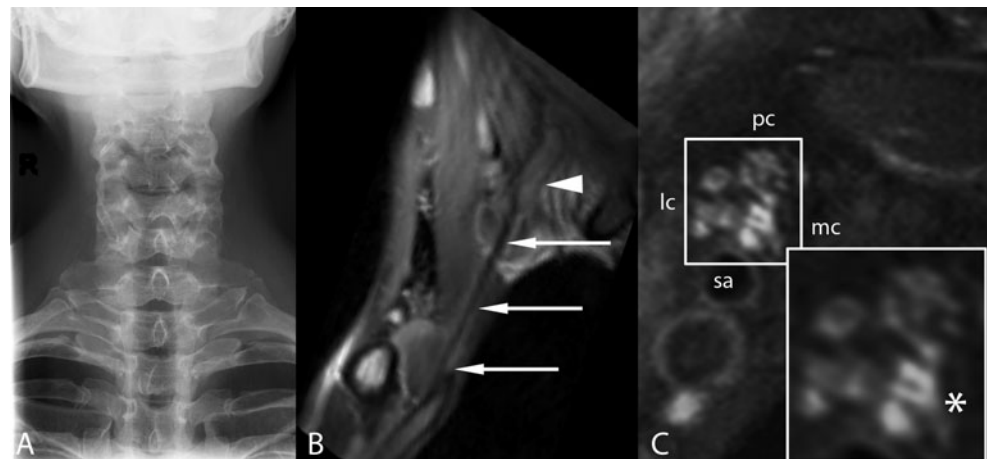
In addition to the described anatomical structures compressing the brachial plexus, the presence of a T2W abnormality within the affected spinal nerves or inferior trunk—but sparing other plexus elements—was observed in all patients. Peripheral nerves are normally isointense to slightly hyperintense to muscle. Hyperintensity on T2W indicates some pathological alteration [13] which is not specific for any certain aetiology but highly sensitive to nerve lesions and very precise for their spatial localisation, provided that artefacts such as the magic angle have been excluded [17]. In the case of entrapment neuropathies, an abnormally high T2W signal within a peripheral nerve should be confined to the site of the lesion [14, 15]. In our patients, the presence of a selective T2 lesion in C8 or the inferior trunk substantiated the presumed entrapment as well as the site of the nerve lesion.

Interestingly, morphological correlates were found not only for classic TOS but also for three cases with symptoms of non-specific TOS. These were due to a fibrous band from an elongated transverse process in two cases and due to a synostosis between first and second thoracic rib in another. These morphological substrates, in conjunction with selective T2 lesions in the compromised plexus structures, left no doubt of a morphologically identifiable underlying pathology, which is occasionally disputed for non-specific TOS, as the name “disputed” TOS suggests [6]. MRN identified a clear surgical target

Table 2 Clinical information of patients with positive MRN findings

Patient	Age	Sex	History and symptoms	Clinical examination	Electrophysiological examination
1	49	F	Pain in left upper arm, hypoesthesia in fingertips, temperature-dependent paraesthesiae in arm, weakness of hand.	Atrophy of thenar and hypothenar muscles with severe paresis of intrinsic hand muscles, thumb flexors and thumb abductors.	ENG: proximal axonal sensorimotor lesion of median and ulnar nerves with absent F-waves and sensory potentials. EMG: chronic neurogenic damage in affected muscles.
2	37	F	Supraclavicular pain for 6 years radiating to left arm, weakness and numbness of hand. Surgeries for presumed UNE and CTS.	Atrophy and severe paresis of thenar and hypothenar muscles, moderate paresis of remaining hand muscles and finger extensors. Hypoesthesia predominant in fingers III-V. Roos test positive.	ENG: severe sensorimotor axonal lesion of median and ulnar nerves with absent F-waves and sensory potentials. EMG: chronic neurogenic damage in affected muscles.
3	20	F	Intermittent pain in neck and shoulder radiating to right arm for over 5 years. Paraesthesiae and dystonic movement of hand with subjective weakness after prolonged activity.	No motor or sensory deficits apparent in neurological examination.	Normal findings in extensive electrodiagnostic examinations.
4	57	M	Painless muscle atrophy in left more than right hand, slowly progressive over 10 years. No dysaesthesiae. Multifocal motor neuropathy was initially diagnosed but intravenous immunoglobulin treatment was of no avail.	Atrophy and weakness accentuated in thenar, hypothenar, and intrinsic hand muscles, less pronounced in finger flexors and extensors. No muscle fasciculation. Left hand with decreased temperature and livid coloration.	ENG: severe sensorimotor axonal damage in median and ulnar nerves with loss of F-waves and absent sensory potentials. EMG: severe signs of chronic neurogenic damage in C8, Th1, and to a lesser extent in distal C7 innervated muscles.
5	58	F	Advanced atrophy of thenar, hypothenar muscles, and intrinsic hand muscles. Pain in shoulder but not hand or forearm for past 1 ½ years. Surgeries for CTS and UNE without subsequent improvement.	Atrophy and moderate paresis of thenar, hypothenar, and intrinsic hand muscles. Pain on pressure upon palpable supraclavicular mass.	ENG: severe axonal motor damage of the median and ulnar nerve but no abnormalities of sensory fibres. EMG: chronic neurogenic damage in affected muscles.
6	18	F	Paraesthesiae in right upper arm and shoulder. Transient motor weakness provoked by extending arm above head.	No neurological deficits detected. Pain upon pressure on lower neck above clavicle.	Normal findings in extensive electrodiagnostic examinations.
7	38	F	Severe brachialgia right after slight blunt shoulder trauma. Symptoms initially only activity-dependent but exacerbated to become permanent within following year, leading to insomnia and depression. Multiple analgesic medications including opiates without sufficient pain relief.	Cold and livid coloured right hand, positive Roos Test. No sensorimotor deficits. Supraclavicular compression causing electric irradiating pain in arm.	Normal findings in extensive electrodiagnostic examinations.

Fig. 1 a Radiography proves the presence of bilateral cervical ribs. **b** Reconstructed sagittal PDW SPACE image displays the entire course of a taut fibrous band (arrows) from the cervical rib (arrowhead) to the first thoracic rib, directly situated along the inferior trunk. **c** Sagittal T2W SPAIR displays increased T2W signal extending from the inferior trunk to the medial cord displayed here



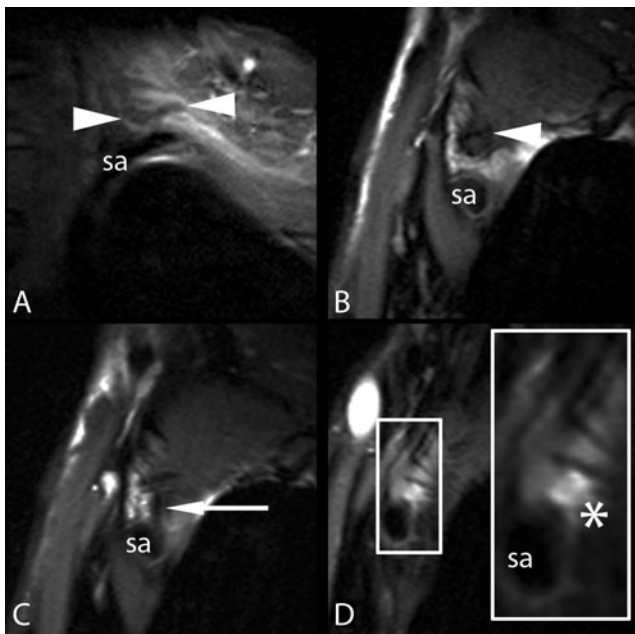


Fig. 2 **a** Elongated transverse process (*arrowheads*) of vertebra C7 in the coronal plane. **b, c** Sagittal T2W SPAIR shows compression of the inferior trunk between an elongated transverse process (*arrowhead*) and the subclavian artery (*sa*) as well as a fibrous band (*arrows*). The exact insertion site of the fibrous band into another rib or the pleura could not be ascertained by imaging in this case. **d** Selective increased T2W signal (*) in those plexus fascicles that become the medial cord. All other plexus structures are normointense

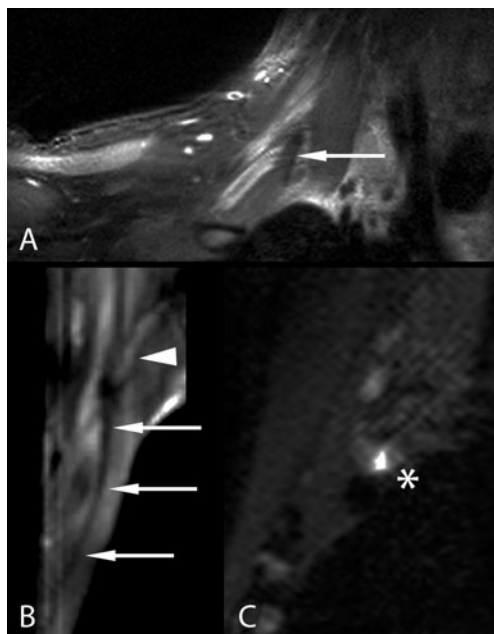


Fig. 3 **a** Coronal reconstructed view in PDW SPACE of the fibrous band (*arrow*) in close proximity to the inferior trunk. **b** Sagittal reconstructed view in PDW SPACE of the fibrous band extending from the cervical rib (*arrowhead*) downwards. **c** Sagittal reconstruction of the 3D SPACE STIR shows increased T2W signal in the C8 spinal nerve (*) and inferior trunk (not on display) directly proximally to the contact with the fibrous band, along with slight calibre increase

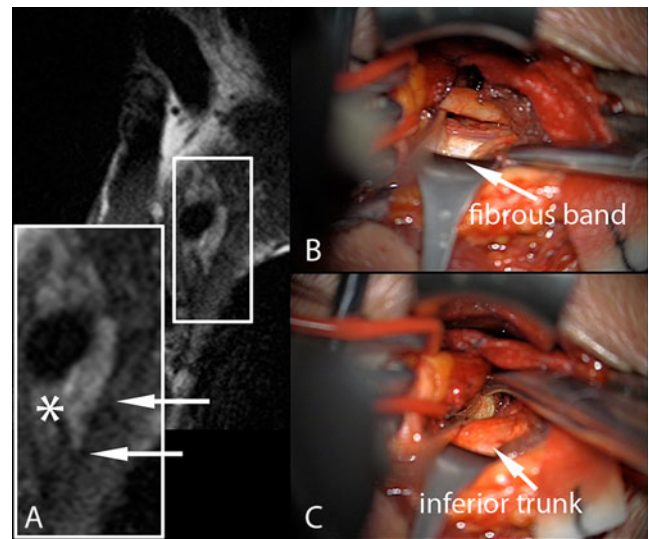


Fig. 4 **a** Sagittal slice of T2W SPAIR shows a thin fibrous band (*arrows*) which originates from an elongated transverse process and compresses the C8 spinal nerve and inferior trunk dorsally. The inferior trunk is swollen (*) with slightly increased T2W signal. **b** Intraoperative preparation of the fibrous band via a supraclavicular approach. Left is medio-caudal, up is medio-cranial. The red vessel loop is on the subclavian artery. **c** View of the swollen inferior trunk after sectioning of the fibrous band and the hypertrophied scalene muscles

in these patients to decompress the brachial plexus, and surgery resulted in pain relief for them. However, the number of patients with negative findings also suggests that there are cases of non-specific TOS without detectable correlate on MRI.

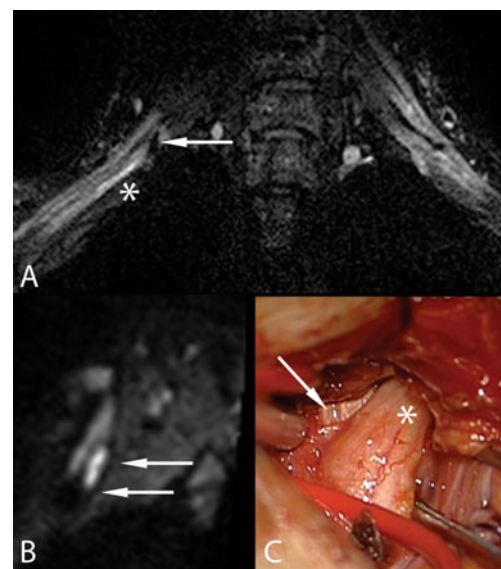


Fig. 5 **a** coronal SPC STIR of the brachial plexus. A T2W lesion of the inferior trunk (*) is observed distal to a hypointense longitudinal structure (*arrow*). **b** Sagittal reconstruction shows this structure to be a fibrous band. Directly ventral to this band is the inferior trunk, which yields high T2W signal, whereas superior and medial trunks appear normal. **c** Surgical exploration confirms a complex compression of the inferior trunk (*), mainly by a thickened fascia of the middle scalene muscle (*arrow*), corresponding to the fibrous band suggested by MRN

A number of limitations apply to this study. Definitive surgical exploration for those patients with negative MRN findings was to our knowledge not performed. We, therefore, cannot determine the number of false-negative findings in MRN. This means that while the method had a positive predictive value of 100 % in our patient group, the negative predictive value remains undetermined. We believe the sensitivity of the method to be high for classic TOS, which also has an electrophysiological correlate of structural nerve damage, and lower for the heterogeneous non-specific TOS. While we did find morphological correlates of TOS in three patients with non-specific TOS, these may not be representative for most patients with non-specific TOS, which may be highly diverse in symptoms, their aetiology and adequate treatment. In the interpretation of images, care must be taken not to misinterpret vascular structures as fibrous bands since they *can* yield similarly hypointense signals. This differentiation is possible by following the course of vascular structures and their eventual entry into larger arteries or veins.

In conclusion, this is the first study of thoracic outlet syndrome in which subtle anatomical anomalies in the course of the brachial plexus, together with T2W abnormalities of the compromised plexus portions, have confirmed the clinical diagnosis. The proposed technique should be of value in the assessment of this diagnostically challenging neurological disease.

Acknowledgments This study was supported by Postdoctoral Fellowships granted to P.B. and M.P. from the Medical Faculty of the University of Heidelberg, and a grant to M.P. and M.B. from the German Osteoarthritis Foundation (Deutsche-Arthrose-Hilfe e.V., Grant number P215-A482).

References

- Povlsen B, Belzberg A, Hansson T, Dorsi M (2010) Treatment for thoracic outlet syndrome. *Cochrane Database Syst Rev* 1, CD007218
- Thomas HM, Cushing HG (1903) Exhibition of two cases of radicular paralysis of the brachial plexus. One from the pressure of a cervical rib with operation. The other of uncertain origin. *Johns Hopkins Hosp Bull* (14):315–319
- Roos DB (1976) Congenital anomalies associated with thoracic outlet syndrome. Anatomy, symptoms, diagnosis, and treatment. *Am J Surg* 132:771–778
- Wilbourn AJ (2005) Brachial plexus lesions. In: Dyck PJ, Thomas PK (eds) *Peripheral neuropathy*. Elsevier Saunders, Philadelphia, pp 1359–1360
- Mackinnon SE, Novak CB (2002) Thoracic outlet syndrome. *Curr Probl Surg* 39:1070–1145
- Ferrante MA (2012) The thoracic outlet syndromes. *Muscle Nerve* 45:780–795
- Stanton PE Jr, Vo NM, Haley T, Shannon J, Evans J (1988) Thoracic outlet syndrome: a comprehensive evaluation. *Am Surg* 54:129–133
- Bilbey JH, Muller NL, Connell DG, Luoma AA, Nelems B (1989) Thoracic outlet syndrome: evaluation with CT. *Radiology* 171:381–384
- Redenbach DM, Nelems B (1998) A comparative study of structures comprising the thoracic outlet in 250 human cadavers and 72 surgical cases of thoracic outlet syndrome. *Eur J Cardiothorac Surg* 13:353–360
- Brewin J, Hill M, Ellis H (2009) The prevalence of cervical ribs in a London population. *Clin Anat* 22:331–336
- Filler AG, Howe FA, Hayes CE et al (1993) Magnetic resonance neurography. *Lancet* 341:659–661
- Filler AG, Kliot M, Howe FA et al (1996) Application of magnetic resonance neurography in the evaluation of patients with peripheral nerve pathology. *J Neurosurg* 85:299–309
- Bendszus M, Stoll G (2005) Technology insight: visualizing peripheral nerve injury using MRI. *Nat Clin Pract Neurol* 1:45–53
- Baumer P, Dombert T, Staub F et al (2011) Ulnar neuropathy at the elbow: MR neurography—nerve T2 signal increase and caliber. *Radiology* 260:199–206
- Baumer P, Weiler M, Ruetters M et al (2012) MR neurography in ulnar neuropathy as surrogate parameter for the presence of disseminated neuropathy. *PLoS One* 7:e49742
- Stoll G, Bendszus M, Perez J, Pham M (2009) Magnetic resonance imaging of the peripheral nervous system. *J Neurol* 256:1043–1051
- Kastel T, Heiland S, Baumer P, Bartsch AJ, Bendszus M, Pham M (2011) Magic angle effect: a relevant artifact in MR neurography at 3T? *AJNR Am J Neuroradiol* 32:821–827